Scientia Iranica, Vol. 10, No. 1, pp 84–90
© Sharif University of Technology, January 2003

SCIENTIA IRANICA

Research Note

Application of Vortex Lattice and Quasi-Vortex Lattice Method with Free Wake in Calculation of Aerodynamic Characteristics of a Hovering Helicopter Rotor Blade in Ground Effect

H. Emdad* and A.H. Nikseresht[1]

In this paper, the aerodynamic characteristics of a rotor blade and its wake effect in hovering flight near the ground are analyzed. The two Methods of Vortex-Lattice (VLM) and Quasi-Vortex-Lattice (QVLM) are employed to model the rotor blade and a free vortex sheet is used to consider the effect of the blade wake. The method of image is employed to predict the ground effect on the aerodynamic characteristics and the wake geometry of a helicopter blade without any restriction on planforms, angle of attack, variable pitch, dihedral angle and camber, as long as stall does not occur. To compute a reasonable and accurate rotor blade wake shape and aerodynamic characteristics in the ground-effect, the effect of the tip and the inboard wake vortices should be modeled precisely. To consider these effects accurately in the ground vicinity, free vortices in the wake are clustered near the tip and trailing-edge, respectively. Also, by reducing the number of turns in the wake from the tip to the root, the effect of the inboard wake vortices will be included and the problem of convergency will be removed. Computed aerodynamic characteristics and wake shape in free flight and in ground-effect compare very well with those of previous numerical and experimental measured data. It should be mentioned that these methods are independent of the initial wake shape, i.e., with any initial wake shape (cylindrical, flat, ...), the problem converges to an identical solution.

INTRODUCTION

The most critical phases in a helicopter flight are takeoff, landing and hovering, in the vicinity of the ground. During takeoff, landing, and hovering near the ground, the aerodynamic and control characteristics of a helicopter are influenced by the proximity of the ground. The phenomenon is called ground effect. When a rotor hovers near the ground, the presence of the ground has a considerable effect on the induced-velocity distribution over the rotor. At ground surface the downwash velocity in the wake is, of course, reduced to zero and this effect is transferred upwards to the disc through pressure changes in the wake, hence, resulting in a lower induced velocity for a given thrust.

Theoretical and experimental research has been devoted to predict helicopter performance in ground effect. Knight and Hefner [1] developed a theoretical treatment to predict helicopter performance in ground effect. They assumed that the circulation along the blade is constant and then the helical tip vortices form a uniform vortex cylinder reaching to the ground. The ground plane is then represented by a reflection of this system, of equal dimensions below the plane but of opposite vorticity, ensuring zero normal velocity at the surface. The work of Zbrozek [2] examined experimental results from many tests and developed an empirical method that was based on rotor height and thrust coefficient. A useful expression emerges from an analysis made by Cheeseman and Bennett [3]. They modeled the rotor as a source and used the method of image to model the ground surface. Hayden [4] developed a simplified empirical model from a large set of flight test data.

Flow visualization can be a very important tool in understanding the physics of the flow field. Taylor [5] examined the flow field of a hovering rotor in ground

*. *Corresponding Author, Department of Mechanical Engineering, University of Shiraz, Shiraz, I.R. Iran.*

1. *Department of Mechanical Engineering, University of Shiraz, Shiraz, I.R. Iran.*

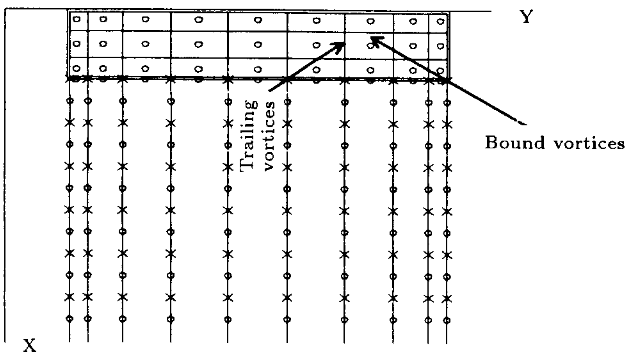

O Control points × Field points

Figure 1. Typical modeling of a blade.

effect using balsa dust particles. Also, Light [6] used the wide-field shadowgraph method to obtain quantitative and qualitative information on the tip vortex geometry of the hovering rotor. Free wake models have been developed for many years which are mainly used for out-of-ground effect [7]. Quackenbush et al. developed the EHPIC (Evaluation of Hover Performance using Influence Coefficient) code [8]. They modeled the rotor blade by using a lifting surface and used curved vortex elements to model the rotor wake. Also, they used the method of imaging to model the effect of the ground. The EHPIC code has a problem of convergence; therefore, to improve the rate of convergence, they fixed the location of inboard vortices. By doing this, the recirculation in the inboard region of the vortex wake in ground effect is not well modeled.

In the present research, a free wake method is used to calculate the wake geometry and performance of an arbitrary blade in the vicinity of the ground. Two methods of vortex lattice (VLM) [9] and quasi vortex lattice (QVLM) [10] are employed to model the rotor blade and a free vortex sheet is used to evaluate the effect of the rotor blade wake (Figure 1). The method of image was employed to predict the ground effect on the aerodynamic characteristics and the wake geometry of a helicopter rotor blade.

In what follows, the formulation of the problem is presented followed by the introduction of the types of boundary conditions and calculation of aerodynamic characteristics. Finally, the results and conclusion are presented.

POTENTIAL FLOW THEORY

As indicated earlier, the present potential flow method is based on the solution of the Prandtl Glauert equation [11]:

$$(1-M_\infty^2)\frac{\partial^2\phi}{\partial x^2}+\frac{\partial^2\phi}{\partial y^2}+\frac{\partial^2\phi}{\partial z^2}=0, \tag{1}$$

where ϕ is the perturbation velocity potential. The solution is presented by vortex distribution and the thin rotor blade approximation is used throughout.

BOUNDARY CONDITIONS

Rotor Blade

The boundary condition for the Prandtl Glauert equation on the rotor blade is that the velocity normal to the blade should be zero. Assume the blade surface can be described as [12]:

$$z=z_c(x,y), \tag{2}$$

where $z_c(x,y)$ is the ordinate of camber surface.

The unit normal vector on the blade surface can be written as:

$$\vec{n}=\frac{-\frac{\partial z_c}{\partial x}\vec{i}-\frac{\partial z_c}{\partial y}\vec{j}+\vec{k}}{\sqrt{1+\left(\frac{\partial z_c}{\partial x}\right)^2+\left(\frac{\partial z_c}{\partial y}\right)^2}}. \tag{3}$$

The total velocity at each point based on the blade surface can be defined as,

$$\vec{V}=\left[(V_\infty\cos\alpha+u)\vec{i}+\nu\vec{j}+(V_\infty\sin\alpha+w)\vec{k}\right], \tag{4}$$

where u,ν and w are the induced velocity components and α is the angle of attack.

Thus, the flow tangency can be satisfied as:

$$\vec{V}.\vec{n}=0\Rightarrow -V_\infty\cos\alpha\left(\frac{\partial z_c}{\partial x}\right)-u\left(\frac{\partial z_c}{\partial x}\right)-\nu\left(\frac{\partial z_c}{\partial y}\right)+V_\infty\sin\alpha+w=0. \tag{5}$$

For describing the above equation in a simpler form, there should be some coordinate transformation. The original $x-y-z$ system is rotated about x-axis through an angle ϕ (dihedral angle), resulting in the $x_1-y_1-z_1$ system and, then, is rotated through an angle α_{tw} (twist angle) about the y_1 axis to result in the $x_2-y_2-z_2$ system. It is shown in [12] that $\frac{\partial z_c}{\partial x}$ and $\frac{\partial z_c}{\partial y}$ can be written as:

$$\frac{\partial z_c}{\partial x}=\frac{-\sin\alpha_{tw}+\frac{d\bar{Z}_c}{dx_2}\cos\alpha_{tw}}{\cos\phi\left(\cos\alpha_{tw}+\frac{d\bar{Z}_c}{dx_2}\cos\alpha_{tw}\right)}, \tag{6}$$

$$\frac{\partial z_c}{\partial y}\approx\tan\phi, \tag{7}$$

where $\frac{d\bar{Z}_c}{dx_2}$ is the camber slope related to its chord axis.

Wake Shape

The vortex segments of the wake are to be aligned in the direction of the local velocity vector calculated at their mid points. However, for better convergence and to avoid numerical fluctuation, it is better that the segments move just a percent of the previous iteration, according to the velocity computed at their mid points. Consider the ith segment of a vortex element. The coordinates of its end points are given by (x_i, y_i, z_i) and $(x_{i+1}, y_{i+1}, z_{i+1})$.

Assume that the velocity at the mid-point of this segment at a given iterative step is given by,

$$\vec{U} = (u\,\vec{i} + \nu\,\vec{j} + w\,\vec{k}), \tag{8}$$

then, it can be written,

$$\Delta x = \frac{\omega u}{U}\Delta s + (1-\omega)(x_{i+1} - x_i)_{\text{old}},$$

$$\Delta y = \frac{\omega \nu}{U}\Delta s + (1-\omega)(y_{i+1} - y_i)_{\text{old}},$$

$$\Delta z = -\sqrt{\Delta s^2 - \Delta y^2 - \Delta x^2}, \tag{9}$$

where ω is the under relaxation factor, which is about $0.7, (x_{i+1} - x_i)_{\text{old}}$ is the x distance of a segment in the previous iteration, and:

$$U = |\vec{U}| = \sqrt{u^2 + \nu^2 + w^2},$$

$$\Delta s = \sqrt{(x_{i+1} - x_i)^2 + (y_{i+1} - y_i)^2 + (z_{i+1} - z_i)^2}.$$

Then, the new location of the $(i+1)$th end point will be:

$$x_{i+1_{\text{New}}} = x_i + \Delta x,$$

$$y_{i+1_{\text{New}}} = y_i + \Delta y,$$

$$z_{i+1_{\text{New}}} = z_i + \Delta z. \tag{10}$$

VORTEX DISTRIBUTION

To satisfy the Prandtl-Glauert Equation 1 and boundary conditions, surface vortex distributions on the rotor blade and the wake are used. According to the Biot-Savart law, the induced velocity at any point $\vec{R}$ in the field is given by [10,13]

$$\vec{V}(\vec{R}) = \frac{\beta^2}{4\pi}\int_s \frac{(\vec{R}_1 - \vec{R}) \times \vec{\gamma}(\vec{R}_1)}{R_\beta^2} ds, \tag{11}$$

where:

$$\vec{R} = x\,\vec{i} + y\,\vec{j} + z\,\vec{k},$$

$$B = \sqrt{(1 - M_\infty^2)},$$

$$R_\beta^2 = (x - x_1)^2 + \beta^2 (y - y_1)^2 + \beta^2 (z - z_1),$$

and $\vec{\gamma}$ is the vorticity vector at $\vec{R}_1 = x_1\,\vec{i} + y_1\,\vec{j} + z_1\,\vec{k}$.

Equation 11 is reduced to a finite sum through the QVLM and VLM. The QVLM methodology was developed to accurately account for mathematical singularities of the square-root type at the leading edges and the Cauchy type in the chordwise integral [10].

GROUND EFFECT

To consider the effect of ground on the rotor blade and wake vortices, the method of image is used. When a rotor blade hovers near ground, the tip vortices do not let the inboard vortices expand, so they come toward the ground and fluctuate. For better convergence, instead of fixing the location of the inboard vortices, as in the EHPIC method, one should only reduce the number of turns of the inboard vortices. By doing this, the effect of the recirculation in the inboard region of the vortex wake in ground effect is modeled. Also, to capture the effect of tip vortices and inboard wake vortices accurately, the free vortices in the wake are clustered in the tip and trailing-edge of the rotor blade, respectively.

SOLUTION PROCEDURE

The problem is nonlinear because the location of the wake and strength of bound vortices are unknown, a priori. To solve the problem, the blade and its image have been segmented into small panels and on each panel a horseshoe vortex and a control point are arranged. Then, the vortex sheet in the wake and its image are discretized. By applying the flow tangency condition on the rotor blade surface, the horseshoe vortex strength is calculated. By satisfying the force free condition on the wake vortex filament, the new location of the vortex sheet is, thus, determined. The above process will be iterated until a converged wake shape and aerodynamic characteristics are obtained. In the following, a brief step by step solution procedure is given [14]:

a) Prescribe the vortex lattice for the blade surface and the initial location of the free elements in the wake;

b) By satisfying the blade boundary condition, obtain the bound vortex density of the blade and the strength of the free elements;

c) Calculate all the aerodynamic characteristics;

d) Adjust the free elements in the wake by satisfying the force free condition;

e) Repeat Steps b through e until a converged solution is obtained.

CALCULATION OF AERODYNAMIC CHARACTERISTICS

The pressure distribution on a rotor blade is calculated by applying the Kutta-Joukowski theorem. There are two types of contribution to the lifting pressure coefficient; one is from the bound vortex filaments and the other from chordwise vortex elements. The ΔC_p, from the bounded element, can be written as [15,16]:

$$(\Delta C_p)_B = 2(u - \nu \tan\psi)\gamma, \tag{12}$$

where u and ν are the total x and y velocity components, ψ is the sweep angle and γ is the strength of the bound vortex. The lifting pressure coefficient from a chordwise vortex filament has the following form [15]:

$$(\Delta C_p)_T = 2\Gamma\nu. \tag{13}$$

Note that the sidewash "ν" is mainly produced by the free vortex filaments. The calculated ΔC_p is interpolated, if necessary, to obtain ΔC_p at integration stations. The calculated pressure force is assumed to be acting normal to the camber surface. This pressure force is then resolved and integrated to obtain the following sectional characteristics [15]:

$$c_l = \frac{1}{c}\int_{x_{LE}}^{x_{TE}} \frac{\Delta C_p\left[\frac{\partial z_c}{\partial x}\sin\alpha + \cos\alpha\right]}{\left[1+\left(\frac{\partial z_c}{\partial x}\right)^2+\left(\frac{\partial z_c}{\partial y}\right)^2\right]^{1/2}}dx, \tag{14}$$

$$c_d = \frac{1}{c}\int_{x_{LE}}^{x_{TE}} \frac{\Delta C_p\left[-\frac{\partial z_c}{\partial x}\cos\alpha + \sin\alpha\right]}{\left[1+\left(\frac{\partial z_c}{\partial x}\right)^2+\left(\frac{\partial z_c}{\partial y}\right)^2\right]^{1/2}}dx, \tag{15}$$

where α is [Nthe angle of attack. The total force coefficient is calculated by a spanwise integration of the sectional force coefficient as:

$$C_L = \frac{1}{s}\int_0^R c_l c\, dy, \tag{16}$$

$$C_D = \frac{1}{s}\int_0^R c_d c\, dy. \tag{17}$$

In hovering flight, the lift and thrust are similar ($T = L$) and the thrust coefficient can be obtained by:

$$C_T = \frac{T}{\pi\rho\Omega^2 R^4}. \tag{18}$$

RESULTS AND DISCUSSIONS

To justify the present developed code, first the aerodynamic characteristics of a rotor blade, with the following configuration and flight conditions, are computed in free flight [17].

This untwisted blade has a radius of 1.14 m and constant chord of 0.19 m, with a root cut-out of 0.188 m at an 8° pitch angle but at different rotating speeds. The first rotor is at 1250 rpm (the tip Mach number as 0.439) and the second at 2050 rpm (the tip Mach number as 0.727). The calculated results are compared with the experimental data of [18] and the boundary integral equation method of [19] in Figures 2 and 3. As is apparent from the figures, the QVLM will show better agreement with the experimental data than the others. There are two reasons for this. One is the elimination of the square root and cauchy type singularities in the leading and trailing edges,

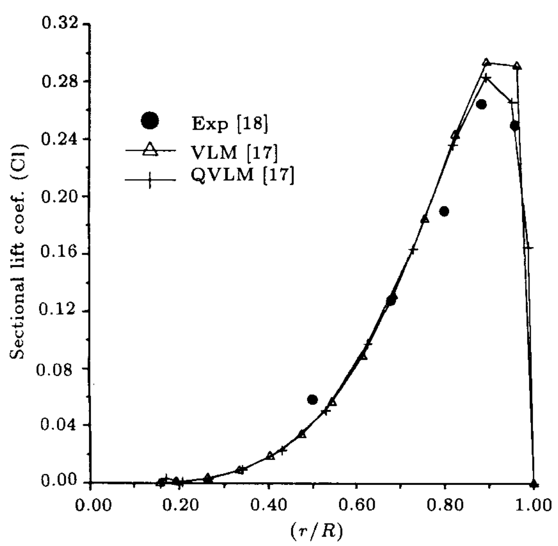

(a) 1250 rpm

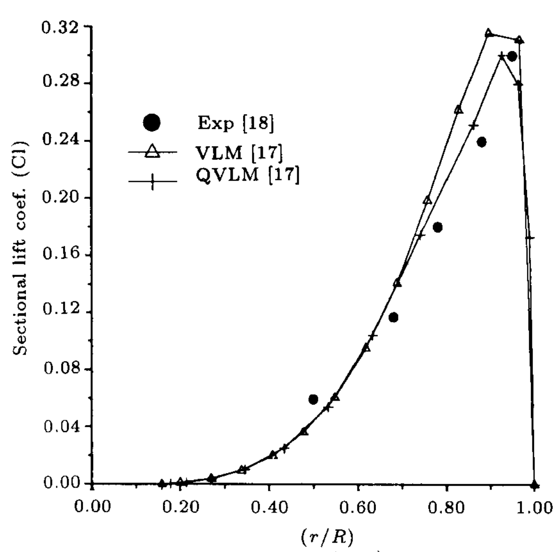

(b) 2050 (rpm)

Figure 2. Sectional lift coefficient versus dimensionless radius.

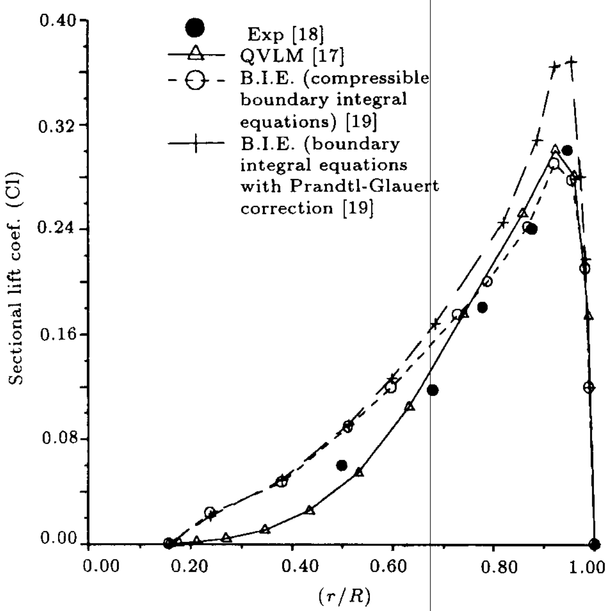

Figure 3. Sectional lift coefficient versus dimensionless radius.

respectively, in the formulation of the QVLM. The other is the clustery of the trailing vortices in the tip region. Also, Figure 4 shows the final wake shape in the free flight for one of the rotor blades.

In the ground effect, computations are performed for the different rotor blade configurations in hovering flight. The following results are focused on a rotor with a rectangular blade and considered at the following geometry and operational parameters as in [6]. This untwisted blade has a constant chord of 0.18 m with a radius of 1.105 m, root cut-out of 0.425 m with a rotating speed of 1645 rpm (the tip Mach number as 0.56).

The VLM and QVLM, with a free wake model, were used to predict the performance and wake shape of the rotor blade in hovering flight, in ground effect. The rotor blade is modeled using three chordwise and eight spanwise panels, while the wake is represented by three turns in the tip and reduced continuously to one turn in the root section, according to the local radius of the blade. The rotor blade aerodynamic characteristics are computed at various heights from the ground plane (H/R, H is the distance of the leading edge from the ground and R is the radius of the rotor blade). The QVLM and VLM calculated ratio of the thrust in ground effect to its value in free flight, versus the height of the blade from the ground are compared with the experimental EHPIC code and the Cheeseman and Bennett relation in Figure 5. Also, it should be noted that in free flight, the value of C_T/σ of the present method, the experimental and EHPIC code are in the range of 0.0155 to 0.019, where σ is the solidity factor. Figure 5 shows that both the VLM and the QVLM have a good agreement with experimental

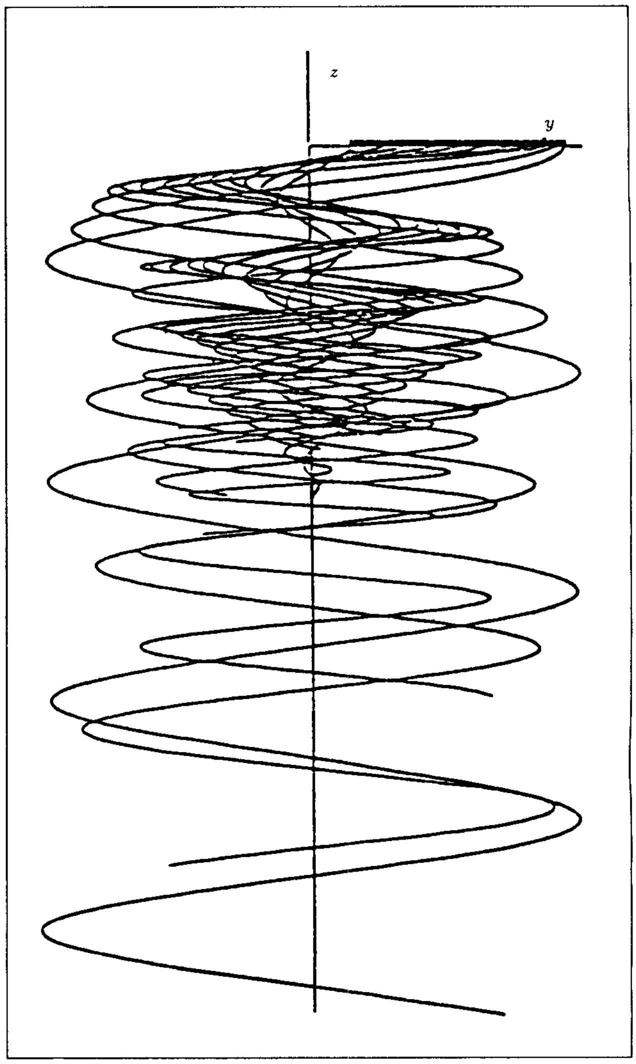

Figure 4. Converged free wake shape with initial cylindrical wake after 15 iterations (QVLM).

data. It is apparent that the correlation of Cheeseman and Bennett [3] over-predicts the results at small heights from the ground plane. This discrepancy was acknowledged in the original development of the method. This method is limited, since it does not take into account the real geometry of the rotor blade (i.e. twist, planform) or operating conditions. The EHPIC method under-predicts the increase in thrust ratio in respect to the experimental measured results. One possible explanation for this, as indicated earlier, may lie in the treatment of the inboard vortex that is not modeled well in their analysis. Also, it is seen that the EHPIC method is restricted to $H/R \cong 0.4$. In the present method, because of the different treatment of the inboard wake vortices, the increase in the thrust ratios is in good agreement with the experimental data (the number of turns of the outboard wake vortices reduced toward the inboard ones). Also, the present method is able to compute the aerodynamic

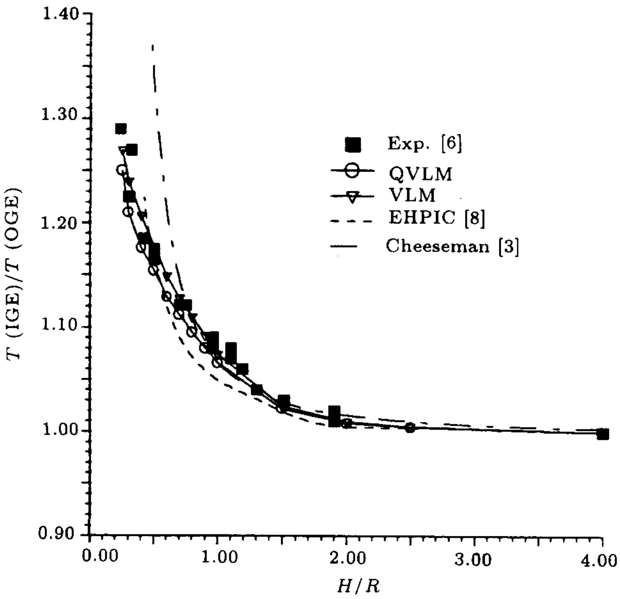

Figure 5. Comparison between VLM, QVLM, EHPIC and Chesseman methods.

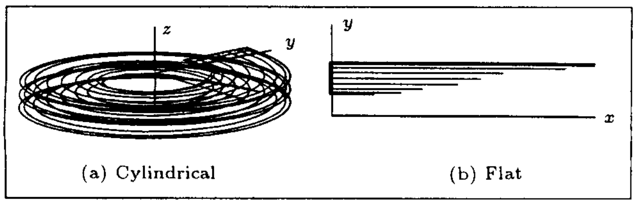

Figure 6. Typical initial free wake shape.

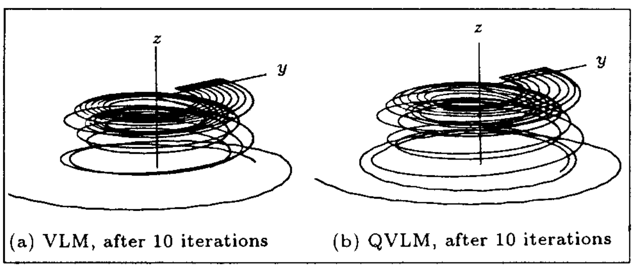

Figure 7. Converged wake shape with initial cylindrical wake ($H/R = 0.8$).

characteristics of the blade rotor closer to the ground (i.e., $H/R \cong 0.23$). In the experiment, because of the unsteady nature of the flow field and the possibility of vortex breakdown, the measured data showed some fluctuation for $H/R \leq 0.3$.

In Figure 6, a typical initial free wake (cylindrical and flat) is shown. Figures 7 and 8 compared the converged wake shape of the VLM with QVLM at two different heights from the ground plane ($H/R = 0.8$ and $H/R = 0.3$). It is apparent that in the QVLM, the tip vortices have a better expansion and, also, are similar to the shadowgraph results of [6] (Figure 10 in [6]).

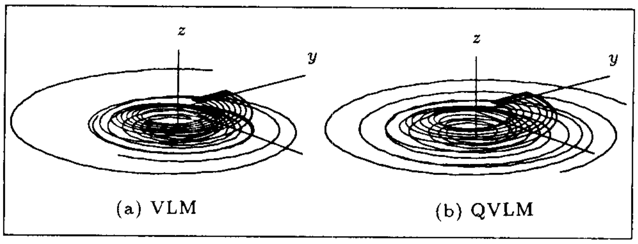

Figure 8. Converged wake shape with initial cylindrical wake after 20 iterations ($H/R = 0.3$).

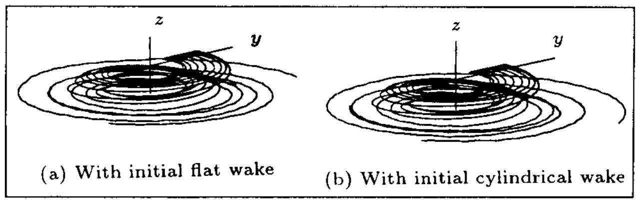

Figure 9. Converged wake shape after 20 iterations with QVLM ($H/R = 0.4$).

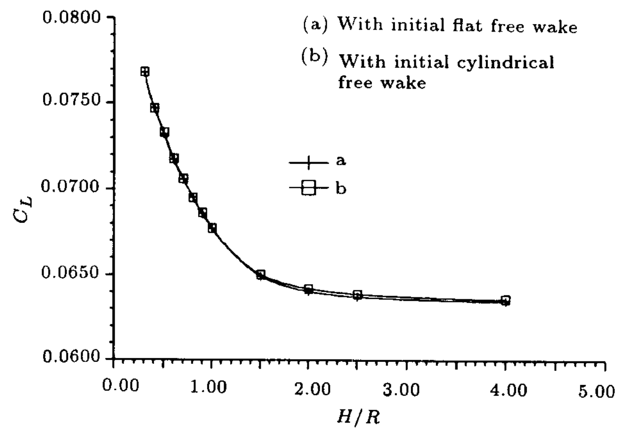

Figure 10. Total lift coefficient versus H/R.

To present the independency of the final wake shape to the initial wake shape, the code is run with an initial flat and cylindrical wake shape in $H/R = 0.4$. Figure 9 shows the final wake shapes with a different initial wake geometry. As evident, the final results are the same. Also, Figures 10 and 11 present the total lift coefficient versus H/R and sectional lift coefficient versus dimensionless radius (r/R) at $H/R = 0.4$. The figures show that for each of the initial wake shapes, there is no difference between the obtained results.

CONCLUSION

Analysis of rotor blades in a hovering motion in the vicinity of the ground has been carried out by QVLM and VLM with a free wake model. The results showed that by reducing the number of turns in the wake from the tip to the root section, the effect of the circulation of the inboard wake vortices would be included. By

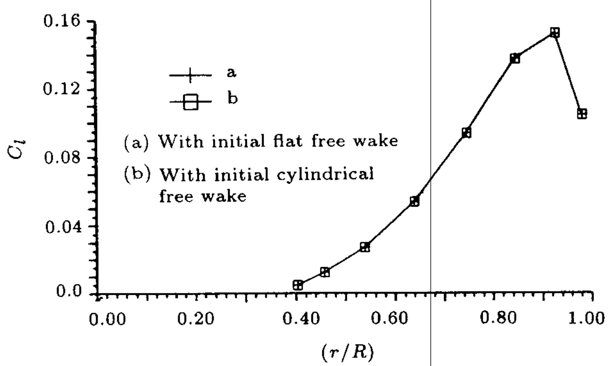

Figure 11. Sectional lift coefficient versus dimensionless radius ($H/R = 0.4$).

clustering the free wake vortices at the tip and trailing-edge of the rotor blade, respectively, the effects of the tip vortices are well modeled. Therefore, the overall aerodynamic characteristics of the rotor blade will be predicted within a good accuracy. Also, QVLM will give much better representation of the tip vortices.

REFERENCES

1. Knight, M. and Hefner, R.A. "Analysis of ground effect on the lifting airscrew", *NACA Tech.*, Note 835 (1941).
2. Zbrozek, J.K. "Ground effect on the lifting rotor", *Rep. Memo. Aeronaut. Res. Coun. 2347* (1947).
3. Cheeseman, I.C. and Bennett, W.E. "The effect of the ground on a helicopter rotor", *ARCR & M 3021* (1955).
4. Hayden, J. "The effect of the ground on helicopter hovering power required", *American Helicopter Society 32nd Annual Forum*, Washington, D.C., USA (May 1976).
5. Taylor, M. "A balsa-dust technique for airflow visualization and its application to flow through model helicopter rotor in static thrust", NACA TN 2220 (Nov. 1950).
6. Light, J.S. "Tip vortex geometry of a hovering helicopter rotor in ground effect", *Journal of American Helicopter Society*, **38**(2), pp 34-42 (Apr. 1993).
7. Quackenbush, T., Bliss, D., Wachspress, D. and Ong, C. "Free wake analysis of hover performance using a new influence coefficient method", NASA CR 4150 (1988).
8. Felker, F., Quackenbush, T., Bliss, D. and Light, J. "Comparisons of predicted and measured rotor performance in hover using a new free wake analysis", *American Helicopter Society 44th Annual Forum*, Washington, D.C., USA (Jun. 1988).
9. Bertine, J.J. and Smith, M.L., *Aerodynamics For Engineers*, Prentice-Hall Inc., USA (1989).
10. Lan, C.E. "A quasi-vortex-lattice method in thin wing theory", *J. of Aircraft*, **11**(9) (1974).
11. Anderson, J.D., *Fundamentals of Aerodynamics*, McGraw-Hill Book Company (1984).
12. Lan, C.E. and Chang, J.F. "Calculation of vortex lift effect for cambered wings by the suction analogy", *Technical Report CRINC-FLR-426-1* (Sep. 1980).
13. Emdad, H. and Hodjati, S.M. "Analysis of rotor with free wake in forward flight using QVLM", *Proceeding of the Second Iranian Conference on Aerospace Engineering*, pp 12-14 (Oct. 1998).
14. Emdad, H. and Lan, C.E. "Wake shape and its effects on aerodynamic characteristics", NASA Contractor Report, 178118 (July 1986).
15. Lan, C.E., Emdad, H., Chin, S., Sundaram, P. and Mehrotra, S. "Calculation of high angle-of-attack aerodynamics of fighter configurations", *AIAA*, pp 89-2188 (1989).
16. Emdad, H., Hodjati, S.M. "Calculation of aerodynamic characteristics of helicopter rotor blade in hover and climb", *Proceeding of the Sixth Annual Mechanical Engineering Conference and Third International Mechanical Engineering Conference of the Iranian Society of Mechanical Engineers*, pp 18-20 (May 1998).
17. Hodjati, S.M. "Analysis of rotor blade and its wake using VLM and QVLM", M.Sc Thesis, Mechanical Eng. Department, Shiraz University (1995).
18. Caradonna, F.X. and Tung, C. "Experimental and analytical studies of a model helicopter rotor in hover", *USAAVRADCOM TR-81-A-23* (1981).
19. Morino, L. and Gennaretti, M., *Boundary Integral Equation Method for Aerodynamics*, The American Institute of Aeronautics and Astronautics (1991).